NUMERICAL MATHEMATICS: Theory, Methods and Applications
Numer. Math. Theor. Meth. Appl., Vol. **2**, No. 1, pp. 18-42 (2009)

Asymptotic Formulas for Thermography Based Recovery of Anomalies

Habib Ammari[1,*], Anastasia Kozhemyak[2] and Darko Volkov[3]

[1] *Laboratoire Ondes et Acoustique, CNRS UMR 7587, ESPCI, 10 rue Vauquelin, 75231 Paris Cedex 05, France.*
[2] *Centre de Mathématiques Appliquées, CNRS UMR 7641, Ecole Polytechnique, 91128 Palaiseau, France.*
[3] *Department of Mathematical Sciences, Worcester Polytechnic Institute, Worcester MA 01609, USA.*

Received 29 April 2008; Accepted (in revised version) 27 August 2008

Abstract. We start from a realistic half space model for thermal imaging, which we then use to develop a mathematical asymptotic analysis well suited for the design of reconstruction algorithms. We seek to reconstruct thermal anomalies only through their rough features. With this way our proposed algorithms are stable against measurement noise and geometry perturbations. Based on rigorous asymptotic estimates, we first obtain an approximation for the temperature profile which we then use to design noniterative detection algorithms. We show on numerical simulations evidence that they are accurate and robust. Moreover, we provide a mathematical model for ultrasonic temperature imaging, which is an important technique in cancerous tissue ablation therapy.

AMS subject classifications: 35R20, 35B30

Key words: Thermography, imaging, asymptotic formulas, small anomalies, direct imaging algorithms, half-space problem.

1. Introduction

Medical thermal imaging has become a procedure of choice in the screening for breast, skin, or liver cancer [10]. It has the ability to identify various stages of disease development, and can pick up early stages which usually elude traditional anatomical examinations. Thermal imaging relies on the fact that chemical and blood vessel activity in pre-cancerous tissue and its surroundings are higher than in healthy tissue. Pre-cancerous and cancerous areas are characterized by heightened metabolism and require an abundant stream of nutrients to maintain growth. These extra nutrients are transported through various channels such as increased chemical activity, enhanced blood stream, and creation

*Corresponding author. *Email addresses:* habib.ammari@espci.fr (H. Ammari), kozhemyak@polytechnique.fr (A. Kozhemyak), darko@wpi.edu (D. Volkov)

of new blood vessels (neoangiogenesis) [15]. This process results in a local increase in temperature.

Detection of these small temperature variations is made possible by state of the art imaging techniques. They involve ultra-sensitive thermal cameras and sophisticated software in detecting, analyzing, and producing high-resolution thermal images of vascular changes. More precisely, medical thermal imaging technique proceeds as follows: an infrared scanning device is used to convert infrared radiation emitted from the skin surface to electrical impulses. Those are then plotted on a color monitor. This map of body surface temperature is referred to as a thermogram. The spectrum of colors corresponds to a scale of infrared radiation emitted from the body surface. Since temperature distribution is highly isotropic in healthy tissue, subtle temperature anisotropies produce a clear imprint. See [1, 13].

Thermal imaging is a very reliable technology. In fact, clinical studies have shown that thermal imaging has an average sensitivity and specificity of 90% when applied to screening of breast tissue. As of today, an abnormal infrared image is the single most important marker of high risk of onset breast cancer. Thermal imaging may also be used for different purposes such as

(i) assessing the extent of a previously diagnosed lesion;

(ii) localizing an abnormal area not previously identified, so further diagnostic tests can be performed;

(iii) detecting early lesions before they are clinically apparent;

(iv) guiding thermal ablation therapies.

In this paper, following an asymptotic formalism in much the same spirit as the recent texts [2, 5], we perform a quantitative study of temperature perturbation due to small thermal anomalies and design algorithms for localizing these anomalies and estimating their size. We start from a realistic model in half space with convective boundary condition on the surface.

Since the exterior temperature is imposed, a convective boundary condition must be used for the model to be physically relevant. Moreover, since the anomalies are expected to be at some distance away from the boundary, the resulting change in surface temperature will be very small: a realistic reconstruction method must take into account inevitable noise blurring of measurements as well as the ill posed nature of the inverse problem. Additionally, we believe that we can realistically assume that the temperature is a known constant far away from the surface: this models temperature far inside the human body, assumed to be constant. In essence, measurements will be made on a planar surface, assumed to be large enough compared to the size of anomalies. In this case a half space formulation provides a viable model. We refer the reader to [7], where such half space formulations are scrutinized.

It is noteworthy that our results can be applied to other types of thermography problems, such as the detection of buried objects in the underground. We seek to reconstruct

only some rough feature of present anomalies. This partial reconstruction has the advantage to be stable against measurement noise and perturbation in geometry. Based on rigorously derived asymptotic estimates, we find an approximation formula that leads us to noniterative detection algorithms for finding dominant features of present anomalies.
We also consider in this paper how to lay the mathematical background for ultrasonic temperature imaging. Ultrasonic temperature imaging is an essential tool for guiding medical devices in the course of thermal ablation therapy. It relies on the fact that sound speed in tissues depends on temperature. Thermal ablation therapy, such as focused ultrasound surgery, is a new way of destroying malignant tumors without damaging surrounding tissue. This technique consists of running the focused ultrasound surgery system at an initial, pre-ablative low intensity while using a diagnostic ultrasound imaging system to detect the associated localized temperature rise. This assumes that the temperature dependence of sound speed is known.

Let us now recall some previous results on anomaly detection by thermal imaging. In a recent paper [4], efficient noniterative algorithms for locating thermal anomalies from boundary measurements of temperature were introduced. The proposed reconstruction was based on a small volume assumption for the anomalies. The authors also assumed that the anomalies lay inside a bounded homogeneous domain, on whose boundary a heat flux was imposed. Resulting temperature was then measured on the same boundary. In another piece of work, Miller et al. [12] studied ultrasonic temperature imaging. Remarkably, their investigation lacks any mathematical analysis. We believe that a rigorous mathematical theory for the effects of thermal anomalies had to be investigated, and that this investigation would help design quantitative analysis methods. Ultimately this study should result in improving accuracy of lesion detection. In the following sections we will first present our novel mathematical analysis, we will then derive reconstruction algorithms. Numerical evidence validating these algorithms is presented in the last section of this paper.

2. Physical background, non-dimensionalisation, Green's function

2.1. Problem statement

We consider the transient heat equation in the half space

$$\Omega = \{(x_1, x_2, x_3) \in \mathbb{R}^3 : x_3 < 0\}$$

in a homogeneous background of thermal conductivity k_0. The background contains regions (of small) volume where the conductivity is different. Denote D the union of all regions where the heat conductivity is different from k_0, and k the over all thermal conductivity function. We define

$$D = \cup_{j=1}^{m} D_j,$$

where the D_j's are such that $k(x)$ is equal to the positive constant k_j on D_j. If we denote τ the temperature function, τ satisfies [9]

$$\frac{\partial \tau}{\partial t} - \nabla \cdot k \nabla \tau = 0 \qquad \text{in } \Omega \text{ and in } (\Omega \setminus \overline{D}) \times (0, T), \tag{2.1}$$

$$\tau^+ = \tau^- \qquad \text{on } \partial D_j \times (0,T), \tag{2.2}$$

$$k_0(\nabla\tau\cdot\nu)^+ = k_j(\nabla\tau\cdot\nu)^- \qquad \text{on } \partial D_j \times (0,T), \tag{2.3}$$

$$\lim_{|x|\to\infty} \tau(x,t) = \tau_0, \tag{2.4}$$

$$\tau(x,0) = \tau_{init}(x), \tag{2.5}$$

$$-k_0\nabla\tau\cdot e_3 = C_{cool}(\tau-\tau_{ext}) \quad \text{on } \partial\Omega\times(0,T), \tag{2.6}$$

where τ_0 is the (constant) temperature at infinity, τ_{init} is the initial temperature profile, and condition (2.6) expresses the radiational cooling on the boundary of Ω. C_{cool} is a positive constant that provides thermal resistance and $\tau_{ext}(x_1,x_2,t)$ is an imposed exterior temperature.

2.2. Non-dimensionalisation

To obtain simpler equations we set

$$u(x,t) = \tau\left(\frac{k_0}{C_{cool}}x, \frac{k_0}{C_{cool}^2}t\right) - \tau_0$$

to obtain the following equations for u:

$$\frac{\partial u}{\partial t} - \Delta u = 0 \qquad \text{in } (\Omega\setminus\overline{D})\times(0,T), \tag{2.7}$$

$$\frac{\partial u}{\partial t} - \nabla\cdot\frac{k}{k_0}\nabla u = 0 \qquad \text{in } D\times(0,T), \tag{2.8}$$

$$u^+ = u^- \text{ on } \partial D_j\times(0,T), \tag{2.9}$$

$$(\nabla u\cdot\nu)^+ = \frac{k_j}{k_0}(\nabla u\cdot\nu)^- \qquad \text{on } \partial D_j\times(0,T), \tag{2.10}$$

$$\lim_{|x|\to\infty} u(x,t) = 0, \tag{2.11}$$

$$u(x,0) = \tau_{init}\Big(\frac{k_0}{C_{cool}}x\Big) - \tau_0 =: u_{init}, \tag{2.12}$$

$$\frac{\partial u}{\partial x_3} + u = \tau_{ext}\Big(\frac{k_0}{C_{cool}}x, \frac{k_0}{C_{cool}^2}t\Big) - \tau_0 := u_{ext} \quad \text{on } \partial\Omega\times(0,T). \tag{2.13}$$

2.3. Existence, uniqueness and continuous dependence on initial data and boundary condition

From general PDE theory, an existence, uniqueness and continuous dependence on initial data and boundary condition result can be stated for the system (2.7)-(2.13).

Theorem 2.1. *Assume $u_{init} \in L^2(\Omega)$, $u_{ext} \in L^2(0,T;L^2(\partial\Omega))$, $f \in L^2(0,T;L^2(\Omega))$. There is a unique weak solution to the following problem:*

$$\frac{\partial u}{\partial t} - \nabla \cdot \frac{k}{k_0}\nabla u = f \qquad \text{in } \Omega \times (0,T), \tag{2.14}$$

$$u(x,0) = u_{init}, \tag{2.15}$$

$$\frac{\partial u}{\partial x_3} + u = u_{ext} \qquad \text{on } \partial\Omega \times (0,T). \tag{2.16}$$

This solution satisfies the estimates

$$\|u\|_{L^2(0,T;H^1(\Omega))} \leq C\left(\|u_{init}\|_{L^2(\Omega)} + \|u_{ext}\|_{L^2(0,T;L^2(\partial\Omega))} + \|f\|_{L^2(0,T;L^2(\Omega))}\right), \tag{2.17}$$

where C is a positive constant depending only on the two positive constants

$$m_1 := \min \frac{k}{k_0}, \quad m_2 := \max \frac{k}{k_0}.$$

Proof. The bilinear functional

$$a(u,v) = \int_\Omega \frac{k}{k_0}\nabla u \nabla v + \int_{\partial\Omega} uv,$$

defined on $H^1(\Omega) \times H^1(\Omega)$ satisfies

$$|a(u,v)| \leq (1+m_2)\|u\|_{H^1(\Omega)}\|v\|_{H^1(\Omega)}, \quad |a(u,u)| \geq m_1\|u\|^2_{H^1(\Omega)} - m_1\|u\|^2_{L^2(\Omega)}.$$

Define the continuous linear functional L on $H^1(\Omega)$ by

$$L(v) = \int_\Omega f(x,t)v(x)dx + \int_{\partial\Omega} u_{ext}(x,t)v(x)dx,$$

for almost all t in $(0,T)$. It follows from, for instance [11, Theorem 1.1, Chapter IV] or [8, Theorem X.9], that the initial value problem

$$a(u(t),v) + \frac{d}{dt}(u(t),v)_{L^2(\Omega)} = (L(u(t)),v)_{H^1(\Omega)',H^1(\Omega)}, \tag{2.18}$$

$$u(0) = u_{init}, \tag{2.19}$$

has a unique solution in $L^2(0,T;H^1(\Omega))$ that depends continuously on L and u_{init}. □

Remark 2.2. We make the following remark on regularity. It is well known that the solution to (2.18)-(2.19) is smooth in $(\Omega \setminus \overline{D}) \times (0,T)$ and in $D \times (0,T)$ provided that f be smooth. Due to [11, Theorem 3.1, Chapter V], if L and u_{init} are more regular, say f is such that

$$\left(\frac{d}{dt}\right)^j f \quad \text{is in} \quad L^2(0,T;H^s_{loc}(\overline{\Omega})) \quad \text{for} \quad j = 0,\cdots,p,$$

u_{ext} is such that

$$\Big(\frac{d}{dt}\Big)^j u_{ext} \quad \text{is in} \quad L^2(0,T;H^{s+\frac{1}{2}}_{loc}(\partial\Omega)) \quad \text{for} \quad j=0,\cdots,p+1,$$

and u_{init} is in $H^{s+2}_{loc}(\overline{\Omega})$, then u is such that

$$\Big(\frac{d}{dt}\Big)^j u \quad \text{is in} \quad L^2(0,T;H^{s+2}_{loc}(\overline{\Omega}\setminus\overline{D})) \quad \text{for} \quad j=0,\cdots,p+1$$

provided the compatibility conditions:

$$\Big(\frac{\partial}{\partial x_1}\Big)^{s_1}\Big(\frac{\partial}{\partial x_2}\Big)^{s_2}\Big(\frac{\partial u_{init}}{\partial x_3}+u_{init}\Big)=\lim_{t\to 0}\Big(\frac{\partial}{\partial x_1}\Big)^{s_1}\Big(\frac{\partial}{\partial x_2}\Big)^{s_2}(u_{ext}) \quad \text{on } \partial\Omega,$$

for $0\le s_1+s_2\le s$, are satisfied.

2.4. Green's function and solution to the unperturbed problem

Setting

$$g(x_1,\xi_1,t)=\frac{1}{2\sqrt{\pi t}}\Big(e^{-\frac{(x_1-\xi_1)^2}{4t}}+e^{-\frac{(x_1+\xi_1)^2}{4t}} - 2\int_0^\infty \exp\Big(-\frac{(x_1+\xi_1+\eta)^2}{4t}-\eta\Big)d\eta\Big) \tag{2.20}$$

it is known that g satisfies (see Sommerfeld's long rod solution [14])

$$\begin{aligned}&\partial_t g=\partial^2_{x_1}g && \text{if } t>0,\xi\neq x \text{ and } \xi\neq -x,\\ &\partial_{x_1}g-g=0 && \text{at } x_1=0, \text{ for } t>0,\end{aligned}$$

and g is a fundamental solution to the heat equation in the rod, in the sense that the function defined by

$$\int_0^t\int_0^\infty f(\xi_1,s)g(x_1,\xi_1,t-s)\,d\xi_1 ds$$

is 0 at time 0, and satisfies $(\partial_t-\partial^2_{x_1}).=f$ in $(0,\infty)^2$ and $\partial_{x_1}\cdot -\cdot=0$ at $x_1=0$, for $t>0$, if f is smooth.

Based on g we construct two Green's functions adapted to our problem

$$G_1(x_1,x_2,x_3,\xi_1,\xi_2,\xi_3,t)=\frac{1}{(2\sqrt{\pi t})^3}e^{-\frac{(x_1-\xi_1)^2+(x_2-\xi_2)^2}{4t}}\Big(e^{-\frac{(x_3-\xi_3)^2}{4t}}+e^{-\frac{(x_3+\xi_3)^2}{4t}} - 2\int_0^\infty \exp\Big(-\frac{(-x_3-\xi_3+\eta)^2}{4t}-\eta\Big)d\eta\Big),$$

$$G_2(x_1,x_2,x_3,\xi_1,\xi_2,t)=G_1(x_1,x_2,x_3,\xi_1,\xi_2,0,t).$$

Note that the integral term in G_1 can be re- expressed as

$$-2\int_0^\infty \exp\Big(-\frac{(-x_3-\xi_3+\eta)^2}{4t}-\eta\Big)d\eta = -2\sqrt{\pi t}e^{-x_3-\xi_3+t}\operatorname{erfc}\Big(\frac{2t-x_3-\xi_3}{2\sqrt{t}}\Big),$$

where erfc is the complementary error function. If we define

$$u_1(x_1,x_2,x_3,t) = \int_{-\infty}^0\int_{-\infty}^\infty\int_{-\infty}^\infty f_1(\xi)G_1(x,\xi,t)d\xi, \tag{2.21}$$

$$u_2(x_1,x_2,x_3,t) = \int_0^t\int_{-\infty}^\infty\int_{-\infty}^\infty f_2(\xi_1,\xi_2,s)G_2(x,\xi_1,\xi_2,t-s)d\xi_1 d\xi_2 ds, \tag{2.22}$$

where $\xi := (\xi_1,\xi_2,\xi_3)$ and $x := (x_1,x_2,x_3)$, then u_1 satisfies

$$\partial_t u_1 - \Delta u_1 = 0 \qquad \text{in } \Omega\times(0,\infty), \tag{2.23}$$

$$\partial_{x_3} u_1 + u_1 = 0 \qquad \text{on } \partial\Omega\times(0,\infty), \tag{2.24}$$

$$u_1(x_1,x_2,x_3,0) = f_1(x_1,x_2,x_3), \tag{2.25}$$

and u_2 satisfies

$$\partial_t u_2 - \Delta u_2 = 0 \qquad \text{in } \Omega\times(0,\infty), \tag{2.26}$$

$$\partial_{x_3} u_2 + u_2 = f_2 \qquad \text{on } \partial\Omega\times(0,\infty), \tag{2.27}$$

$$u_2(x_1,x_2,x_3,0) = 0. \tag{2.28}$$

Consequently if the thermal conductivity k is constant throughout Ω (or equivalently the set D is empty) problem (2.7)-(2.13) can be solved by convolution. The solution, denoted by u_0 in that case, is given by

$$\begin{aligned} u_0(x_1,x_2,t) = &\int_{-\infty}^0\int_{-\infty}^\infty\int_{-\infty}^\infty u_{init}(\xi)G_1(x,\xi,t)d\xi_1 d\xi_2 d\xi_3 \\ &+\int_0^t\int_{-\infty}^\infty\int_{-\infty}^\infty u_{ext}(\xi_1,\xi_2,s)G_2(x,\xi_1,\xi_2,t-s)d\xi_1 d\xi_2 ds. \end{aligned} \tag{2.29}$$

Remark 2.3. Eqs. (2.23)-(2.25) assume some regularity on f_1. For example (2.23)-(2.24) are satisfied if f_1 is in $L^2(\Omega)$ and for (2.25) to be satisfied at a fixed point x we may require

$$\lim_{\varepsilon\to 0}\int_{|y|\le\varepsilon}|f_1(x+y)-f_1(x)|dy = 0.$$

Obtaining Eqs. (2.26)-(2.28) from (2.22) is not standard: we provide a proof in the appendix. It can be done under the assumptions f_2 is in $L^2(\mathbb{R}^2\times(0,\infty))$ and

$$\lim_{\varepsilon\to 0}\int_{0\le s\le\varepsilon}\int_{|y|\le\varepsilon}|f_2(x+y,t-s)-f_2(x,t)|dyds = 0,$$

for (4.4) to be satisfied at (x,t).

3. The perturbed temperature field

In this section we rigorously derive inner and outer expansions of the perturbations in the temperature field with respect to the size of the anomaly. Our derivations follow those in [4]. However, because of the half-space setting and the convective boundary condition on the surface, some substantial changes are necessary. The arguments of [4] have to be adapted with special care to the more practical setting we are dealing with in this paper. For the reader's convenience, we give a detailed solution to the present problem.

3.1. A preliminary result

We now give a continuous dependence result for a problem similar to (2.7)-(2.16) with special jump conditions across ∂D. The following proposition holds.

Proposition 3.1. *Let D be a region made up of a finite collection of bounded connected smooth domains D_j, strictly included in Ω. Let α be a positive constant less than 1. As previously k is assumed to be equal to the positive constant k_j in D_j and k_0 in $\Omega \setminus D$. There is a unique v in $L^2(0,T;H^1(\Omega))$ satisfying the problem*

$$\frac{\partial v}{\partial t} - \Delta v = F \qquad \text{in } (\Omega \setminus \overline{D}) \times (0,T), \tag{3.1}$$

$$\frac{\partial v}{\partial t} - \nabla \cdot \frac{k}{k_0} \nabla v = F \qquad \text{in } D \times (0,T), \tag{3.2}$$

$$v^+ = v^- \qquad \text{on } \partial D_j \times (0,T), \tag{3.3}$$

$$(\nabla v \cdot \nu)^+ - \frac{k_j}{k_0} (\nabla v \cdot \nu)^- = f \qquad \text{on } \partial D_j \times (0,T), \tag{3.4}$$

$$v(x,0) = v_{init}, \tag{3.5}$$

$$\frac{\partial v}{\partial x_2} + \alpha v = v_{ext} \qquad \text{on } \partial\Omega \times (0,T), \tag{3.6}$$

where F is in $L^2(0,T;L^2(\Omega))$, f is in $L^2(0,T;L^2(\partial D))$, v_{init} is in $L^2(\Omega)$, v_{ext} is in $L^2(0,T;L^2(\partial\Omega))$. Indeed,

$$\begin{aligned} &\|v\|_{L^2(0,T;H^1(\Omega))} \\ &\leq C\Big(\|v_{init}\|_{L^2(\Omega)} + \|v_{ext}\|_{L^2(0,T;L^2(\partial\Omega))} + \|F\|_{L^2(0,T;L^2(\Omega))} + \|f\|_{L^2(0,T;L^2(\partial D))} \Big), \end{aligned} \tag{3.7}$$

where C depends on $\min k/k_0$, $\max k/k_0$ but is independent of $\alpha \leq 1$ and of D.

Proof. Choose the functional L to be

$$L(v) = \int_\Omega F(x,t)v(x)dx + \int_{\partial\Omega} u_{ext}(x,t)v(x)dx + \int_{\partial D} f(x,t)v(x)dx,$$

for almost all t in $(0,T)$, and a to be

$$a(u,v)=\int_\Omega \frac{k}{k_0}\nabla u\nabla v+\alpha\int_{\partial\Omega} uv.$$

It is clear that the proposition is a simple extension of Theorem 2.1. □

3.2. Equations for the perturbed part of the temperature field

We now assume that $D_j=z_j+\varepsilon B_j$, where the z_j's are fixed points and ε is a dilation parameter tending to 0. We denote u_ε the corresponding solution to (2.7)-(2.13). We also assume that u_{init} is in $L^2(\Omega)$ and that and u_{ext} is in $L^2(0,T;L^2(\partial\Omega))$. The difference $v_\varepsilon=u_\varepsilon-u_0$ satisfies the following equations

$$\frac{\partial v_\varepsilon}{\partial t}-\Delta v_\varepsilon=0 \qquad \text{in } (\Omega\setminus\overline{D})\times(0,T), \tag{3.8}$$

$$\frac{\partial v_\varepsilon}{\partial t}-\nabla\cdot\frac{k}{k_0}\nabla v_\varepsilon=\Big(\frac{k}{k_0}-1\Big)\Delta u_0 \qquad \text{in } D\times(0,T), \tag{3.9}$$

$$v_\varepsilon^+=v_\varepsilon^- \qquad \text{on } \partial D_j\times(0,T), \tag{3.10}$$

$$(\nabla v_\varepsilon\cdot\nu)^+-\frac{k_j}{k_0}(\nabla v_\varepsilon\cdot\nu)^-=\Big(\frac{k}{k_0}-1\Big)\nabla u_0\cdot\nu \qquad \text{on } \partial D_j\times(0,T), \tag{3.11}$$

$$\lim_{|x|\to\infty} v_\varepsilon(x,t)=0,\quad v_\varepsilon(x,0)=0, \tag{3.12}$$

$$\frac{\partial v_\varepsilon}{\partial x_3}+v_\varepsilon=0 \qquad \text{on } \partial\Omega\times(0,T), \tag{3.13}$$

where u_0 is given by (2.29). As u_0 is smooth in a neighborhood of D in the time interval (η,T) for $0<\eta<T$, Eqs. (3.8)-(3.13) imply due to Proposition 3.1 that

$$\|v_\varepsilon\|_{L^2(0,T;H^1(\Omega))}\le CT^{\frac{1}{2}}\varepsilon.$$

3.3. The correction term

As in [4], set

$$V=v_\varepsilon+\varepsilon\sum_{j=1}^{m}\sum_{i=1}^{3}\partial_{x_i}u_0(z_j,t)\psi_{j,i}\Big(\frac{x-z_j}{\varepsilon}\Big),$$

where $\psi_{j,i}$ satisfies

$$\Delta\psi_{j,i}=0 \text{ in } B_j \text{ and in } \mathbb{R}^3\setminus\overline{B_j},\quad \psi_{j,i} \text{ is continuous across } \partial B_j,$$

$$(\partial_\nu\psi_{j,i})^+-\frac{k}{k_0}(\partial_\nu\psi_{j,i})^-=\Big(1-\frac{k}{k_0}\Big)\partial_\nu x_i,$$

$$\psi_{j,i}(x)=\mathcal{O}\Big(\frac{1}{|x|^2}\Big) \text{ as } |x|\to+\infty.$$

The following result holds.

Theorem 3.2. *There exists a positive constant C independent of T and ε such that*

$$\|V\|_{L^2(0,T;H^1(\Omega))} \leq CT^{\frac{1}{2}}\varepsilon^{\frac{5}{2}}.$$

Proof. For the sake of simpler notations we assume in this proof that $m = 1$. We first perform a rescaling by setting $v(x,t) = V(\varepsilon x, \varepsilon^2 t)$. Then v satisfies (3.1)-(3.6) with $m = 1$ and

$$\begin{aligned}
F(x,t) &= \varepsilon^3 \sum_{i=1}^{3} (\partial_{x_i}\partial_t u_0)(z_1, \varepsilon^2 t)\psi_i\Big(x - \frac{z_1}{\varepsilon}\Big), \quad \text{in } \Omega \setminus \Big(\frac{z_1}{\varepsilon} + B_1\Big) \times (0, T/\varepsilon^2),\\
F(x,t) &= \varepsilon^3 \sum_{i=1}^{3} (\partial_{x_i}\partial_t u_0)(z_1, \varepsilon^2 t)\psi_i\Big(x - \frac{z_1}{\varepsilon}\Big)\\
&\quad + \varepsilon^2\Big(\frac{k}{k_0} - 1\Big)(\Delta u_0)(\varepsilon x, \varepsilon^2 t), \quad \text{in } \Big(\frac{z_1}{\varepsilon} + B_1\Big) \times (0, T/\varepsilon^2),\\
f(x,t) &= \varepsilon\Big(\frac{k}{k_0} - 1\Big)(\partial_\nu u_0)(\varepsilon x, \varepsilon^2 t) + \varepsilon \sum_{i=1}^{3} (\partial_{x_i} u_0)(z_1, \varepsilon^2 t)\Big(1 - \frac{k}{k_0}\Big)\partial_\nu x_i,\\
&\quad \text{on } \Big(\frac{z_1}{\varepsilon} + \partial B_1\Big) \times (0, T/\varepsilon^2),\\
v_{init} &= \varepsilon \sum_{i=1}^{3} \partial_i u_0(z_j, 0)\psi_i\Big(x - \frac{z_1}{\varepsilon}\Big),\\
v_{ext} &= \varepsilon \sum_{i=1}^{3} \partial_i u_0(z_j, 0)(\partial_{x_3}\psi_i)\Big(x - \frac{z_1}{\varepsilon}\Big) + \varepsilon^2 \sum_{i=1}^{3} \partial_i u_0(z_j, 0)\psi_i\Big(x - \frac{z_1}{\varepsilon}\Big),\\
&\quad \text{on } \partial\Omega, \text{ with the choice } \alpha = \varepsilon.
\end{aligned}$$

It is easily seen that

$$\|F(x,t)\|^2_{L^2(\Omega)} \leq C\varepsilon^4.$$

Consequently,

$$\|F(x,t)\|^2_{L^2(0,T/\varepsilon^2;L^2(\Omega))} \leq CT\varepsilon^2. \tag{3.14}$$

Next, we estimate f. We set $y = x - z_1/\varepsilon$. That way

$$\begin{aligned}
f(x,t) = f\Big(y + \frac{z_1}{\varepsilon}, t\Big) &= \varepsilon\Big(\frac{k}{k_0} - 1\Big)(\partial_\nu u_0)(\varepsilon y + z_1, \varepsilon^2 t)\\
&\quad + \varepsilon \sum_{i=1}^{3} (\partial_{x_i} u_0)(z_1, \varepsilon^2 t)\Big(1 - \frac{k}{k_0}\Big)\partial_\nu y_i, \quad \text{for } y \text{ on } (\partial B_1) \times (0, T/\varepsilon^2),
\end{aligned}$$

and using the fact that u_0 is smooth in $\Omega \times (0,T)$, we see that f is bounded in the sup norm by $C\varepsilon^2$, from which it follows that

$$\|f(x,t)\|^2_{L^2(\partial B_1)} \leq C\varepsilon^4.$$

Consequently,

$$\|f(x,t)\|^2_{L^2(0,T/\varepsilon^2;L^2(\partial B_1))} \leq CT\varepsilon^2. \tag{3.15}$$

It is also clear that

$$\|v_{init}\|^2_{L^2(\Omega)} \leq C\varepsilon^2. \tag{3.16}$$

Finally, we estimate v_{ext}. Denote (z_{11}, z_{12}, z_{13}) the coordinates of z_1. For $x = (x_1, x_2, 0)$ on $\partial\Omega$

$$\left|x - \frac{z_1}{\varepsilon}\right|^2 = \left(x_1 - \frac{z_{11}}{\varepsilon}\right)^2 + \left(x_2 - \frac{z_{12}}{\varepsilon}\right)^2 + \left(\frac{z_{13}}{\varepsilon}\right)^2.$$

We find due to the decay of $(\partial_{x_3}\psi_{j,i})$ that

$$\|(\partial_{x_3}\psi_i)(x - z_1/\varepsilon)\|^2_{L^2(\partial\Omega)} \leq C\int_0^\infty \frac{\rho d\rho}{\rho^6 + (z_{13}/\varepsilon)^6} \leq C\varepsilon^4,$$

and due to the decay of $\psi_{j,i}$ that

$$\|\psi_i(x - z_1/\varepsilon)\|^2_{L^2(\partial\Omega)} \leq C\int_0^\infty \frac{\rho d\rho}{\rho^4 + (z_{13}/\varepsilon)^4} \leq C\varepsilon^2.$$

We infer,

$$\|v_{ext}\|^2_{L^2(\partial\Omega)} \leq C\varepsilon^6.$$

Consequently,

$$\|v_{ext}\|^2_{L^2(0,T/\varepsilon^2;L^2(\partial\Omega))} \leq CT\varepsilon^4. \tag{3.17}$$

We now apply (3.7) to obtain that

$$\|v(x,t)\|^2_{L^2(0,T/\varepsilon^2;H^1(\Omega))} \leq CT\varepsilon^2$$

and changing variables yields

$$\|V(x,t)\|^2_{L^2(0,T;L^2(\Omega))} \leq \varepsilon^5\|v(x,t)\|^2_{L^2(0,T/\varepsilon^2;L^2(\Omega))} \leq CT\varepsilon^7,$$
$$\|\nabla_x V(x,t)\|^2_{L^2(0,T;L^2(\Omega))} \leq \varepsilon^3\|\nabla_x v(x,t)\|^2_{L^2(0,T/\varepsilon^2;L^2(\Omega))} \leq CT\varepsilon^5,$$

as desired. □

4. The two-dimensional case

Section 2 can be adjusted to a two-dimensional model by making a few straightforward modifications. We make these adjustments explicit only for the expression for the Green's function for the homogeneous problem. Adjusting Section 2 is less obvious and will require the introduction of a cut off function.

4.1. Straightforward modifications of Green's function to fit the 2D case

Based on g defined in (2.20) we construct two Green's functions adapted to our problem

$$G_1(x_1,x_2,\xi_1,\xi_2,t)=\frac{1}{4\pi t}e^{-\frac{(x_1-\xi_1)^2}{4t}}\Big(e^{-\frac{(x_2-\xi_2)^2}{4t}}+e^{-\frac{(x_2+\xi_2)^2}{4t}} \\ -2\int_0^\infty \exp\Big(-\frac{(-x_2-\xi_2+\eta)^2}{4t}-\eta\Big)d\eta\Big),$$

and

$$G_2(x_1,x_2,\xi_1,t)=G_1(x_1,x_2,\xi_1,0,t).$$

If we define

$$u_1(x_1,x_2,t)=\int_{-\infty}^{\infty}\int_{-\infty}^{0} f_1(\xi_1,\xi_2)G_1(x_1,x_2,\xi_1,\xi_2,t)d\xi_2 d\xi_1, \tag{4.1}$$

$$u_2(x_1,x_2,t)=\int_0^t\int_{-\infty}^{\infty} f_2(\xi_1,s)G_2(x_1,x_2,\xi_1,t-s)d\xi_1 ds. \tag{4.2}$$

Then u_1 satisfies

$$\begin{aligned}&\partial_t u_1-\Delta u_1=0 \ \text{ in } \Omega\times(0,\infty),\\ &\partial_{x_2}u_1+u_1=0 \ \text{ on } \partial\Omega\times(0,\infty),\\ &u_1(x_1,x_2,0)=f_1(x_1,x_2),\end{aligned}$$

and u_2 satisfies

$$\partial_t u_2-\Delta u_2=0 \ \text{ in } \Omega\times(0,\infty), \tag{4.3}$$

$$\partial_{x_2}u_2+u_2=f_2 \ \text{ on } \partial\Omega\times(0,\infty), \tag{4.4}$$

$$u_1(x_1,x_2,0)=0. \tag{4.5}$$

Consequently, if the thermal conductivity k is constant throughout Ω (or equivalently the set D is empty) problem (2.7)-(2.13) can be solved by convolution. The solution, denoted u_0 in that case is given by

$$u_0(x_1,x_2,t)=\int_{-\infty}^{\infty}\int_{-\infty}^{0} u_{init}(\xi_1,\xi_2)G_1(x_1,x_2,\xi_1,\xi_2,t)d\xi_2 d\xi_1 \\ +\int_0^t\int_{-\infty}^{\infty} u_{ext}(\xi_1,s)G_2(x_1,x_2,\xi_1,t-s)d\xi_1 ds.$$

4.2. Special corrector obtained by introducing a cut off function

The definition of the difference v_ε between the homogeneous and perturbed heat profiles is the same in the two dimensional case: Eqs. (3.8)-(3.13) apply in that case too. Proposition 3.1 may be used as well in the two dimensional case. It is the insufficiently rapid decay of $\psi_{j,i}$ at infinity that makes the two dimensional case distinct, as explained further down. Let $\psi_{j,i}$ satisfy

$$\begin{aligned}
&\Delta\psi_{j,i} = 0 \ \text{ in } B_j \text{ and in } \mathbb{R}^2 \setminus \overline{B_j},\\
&\psi_{j,i} \ \text{ is continuous across } \partial B_j,\\
&(\partial_\nu \psi_{j,i})^+ - \frac{k}{k_0}(\partial_\nu \psi_{j,i})^- = (1-k/k_0)\partial_\nu x_i,\\
&\psi_{j,i}(x) = \mathcal{O}(|x|^{-1}) \ \text{ as } |x| \to +\infty.
\end{aligned}$$

As a closed form expression for $\psi_{j,i}$ in the case where B_j is the unit disk centered at the origin is given by

$$\begin{aligned}
\psi_{j,i}(x) &= \frac{k_0-k}{k_0+k}x_i \qquad \text{in } B_j,\\
\psi_{j,i}(x) &= \frac{k_0-k}{k_0+k}\frac{x_i}{|x|^2} \qquad \text{in } \mathbb{R}^2 \setminus \overline{B_j},
\end{aligned}$$

we conclude that $\psi_{j,i}(x)$ is not in $L^2(\mathbb{R}^2)$ in that case. Fix a function ρ in $\mathscr{C}^\infty(\mathbb{R}^2)$ such that

$$\rho(x) = 1 \ \text{ if } |x| \le 1, \quad \rho(x) = 0 \ \text{ if } |x| \ge 2.$$

Set

$$V = v_\varepsilon + \varepsilon \sum_{j=1}^{m}\sum_{i=1}^{2} \partial_{x_i} u_0(z_j,t)\psi_{j,i}\Big(\frac{x-z_j}{\varepsilon}\Big)\rho(\varepsilon x). \tag{4.6}$$

Notice that

$$\Big\|\psi_{j,i}\Big(\frac{x-z_j}{\varepsilon}\Big)\rho(\varepsilon x)\Big\|^2_{L^2(\Omega)} \le C\varepsilon^2|\log\varepsilon|.$$

4.3. Derivation of the order of the estimate

Our main result is the following theorem.

Theorem 4.1. *There exists a positive constant C independent of T and ε such that*

$$\|V\|_{L^2(0,T;H^1(\Omega))} \le C T^{\frac{1}{2}} \varepsilon^2 |\log\varepsilon|^{\frac{1}{2}},$$

for the two-dimensional case.

Proof. For the sake of simpler notations we assume that $m = 1$. First we rescale $v(x,t) = V(\varepsilon x, \varepsilon^2 t)$. v satisfies (3.1)-(3.6) with $m = 1$ and

$$F(x,t) = \varepsilon^3 \sum_{i=1}^{2} (\partial_{x_i}\partial_t u_0)(z_j, \varepsilon^2 t)\psi_i\Big(x - \frac{z_1}{\varepsilon}\Big)\rho(\varepsilon^2 x) + (\partial_{x_i} u_0)(z_j, \varepsilon^2 t)\Big[\nabla\psi_i\Big(x - \frac{z_1}{\varepsilon}\Big)$$
$$\nabla\rho(\varepsilon^2 x) + \varepsilon\psi_i\Big(x - \frac{z_1}{\varepsilon}\Big)\Delta\rho(\varepsilon^2 x)\Big], \quad \text{in } \Omega \setminus \Big(\frac{z_1}{\varepsilon} + B_1\Big) \times (0, T/\varepsilon^2),$$

$$F(x,t) = \varepsilon^3 \sum_{i=1}^{2} (\partial_{x_i}\partial_t u_0)(z_1, \varepsilon^2 t)\psi_i\Big(x - \frac{z_1}{\varepsilon}\Big) + \varepsilon^2\Big(\frac{k}{k_0} - 1\Big)(\Delta u_0)(\varepsilon x, \varepsilon^2 t),$$
$$\text{in } \Big(\frac{z_1}{\varepsilon} + B_1\Big) \times (0, T/\varepsilon^2),$$

$$f(x,t) = \varepsilon\Big(\frac{k}{k_0} - 1\Big)(\partial_\nu u_0)(\varepsilon x, \varepsilon^2 t) + \varepsilon \sum_{i=1}^{2} (\partial_{x_i} u_0)(z_j, \varepsilon^2 t)\Big(1 - \frac{k}{k_0}\Big)\partial_\nu x_i,$$
$$\text{on } \Big(\frac{z_1}{\varepsilon} + \partial B_1\Big) \times (0, T/\varepsilon^2),$$

$$v_{init} = \varepsilon \sum_{i=1}^{2} \partial_i u_0(z_j, 0)\psi_i\Big(x - \frac{z_1}{\varepsilon}\Big)\rho(\varepsilon^2 x),$$

$$v_{ext} = \varepsilon \sum_{i=1}^{2} \partial_i u_0(z_j, 0)(\partial_{x_2}\psi_i)\Big(x - \frac{z_1}{\varepsilon}\Big)\rho(\varepsilon^2 x) + \varepsilon\partial_i u_0(z_j, 0)\psi_i\Big(x - \frac{z_1}{\varepsilon}\Big)(\partial_{x_2}\rho)(\varepsilon^2 x)$$
$$+ \varepsilon^2 \sum_{i=1}^{2} \partial_i u_0(z_j, 0)\psi_i\Big(x - \frac{z_1}{\varepsilon}\Big)\rho(\varepsilon^2 x), \quad \text{on } \partial\Omega \text{ with the choice } \alpha = \varepsilon.$$

It is easily seen that

$$\|F(x,t)\|^2_{L^2(\Omega)} \le C\varepsilon^4 \quad \text{thus} \quad \|F(x,t)\|^2_{L^2(0,T/\varepsilon^2;L^2(\Omega))} \le CT\varepsilon^2. \tag{4.7}$$

Next, using the fact that u_0 is smooth in $\Omega \times (0,T)$, we obtain just as in the three dimensional case

$$\|f(x,t)\|^2_{L^2(\partial B_1)} \le C\varepsilon^4 \quad \text{thus} \quad \|f(x,t)\|^2_{L^2(0,T/\varepsilon^2;L^2(\partial B_1))} \le CT\varepsilon^2. \tag{4.8}$$

It is also clear that

$$\|v_{init}\|^2_{L^2(\Omega)} \le C\varepsilon^2 |\log\varepsilon|. \tag{4.9}$$

Finally we estimate v_{ext}. Denote (z_{11}, z_{12}) the coordinates of z_1. For $x = (x_1, 0)$ on $\partial\Omega$

$$|x - z_1/\varepsilon|^2 = (x_1 - z_{11}/\varepsilon)^2 + (z_{12}/\varepsilon)^2.$$

We find due to the decay of $(\partial_{x_2}\psi_{j,i})$ that

$$\|(\partial_{x_2}\psi_i)(x - z_1/\varepsilon)\rho(\varepsilon^2 x)\|^2_{L^2(\partial\Omega)} \le C\int_0^\infty \frac{d\rho}{\rho^4 + (z_{13}/\varepsilon)^4} \le C\varepsilon^3,$$

and due to the decay of $\psi_{j,i}$ that

$$\|\psi_i(x-z_1/\varepsilon)\partial_{x_2}\rho(\varepsilon^2 x)\|^2_{L^2(\partial\Omega)} \le C\int_0^\infty \frac{d\rho}{\rho^2+(z_{13}/\varepsilon)^2} \le C\varepsilon,$$
$$\|\psi_i(x-z_1/\varepsilon)\rho(\varepsilon^2 x)\|^2_{L^2(\partial\Omega)} \le C\int_0^\infty \frac{d\rho}{\rho^2+(z_{13}/\varepsilon)^2} \le C\varepsilon.$$

We infer,

$$\|v_{ext}\|^2_{L^2(\partial\Omega)} \le C\varepsilon^5 \quad \text{thus} \quad \|v_{ext}\|^2_{L^2(0,T/\varepsilon^2;L^2(\partial\Omega))} \le CT\varepsilon^3. \tag{4.10}$$

We now apply (3.7) to obtain that

$$\|v(x,t)\|^2_{L^2(0,T/\varepsilon^2;H^1(\Omega))} \le CT\varepsilon^2|\log\varepsilon|,$$

and changing variables yields

$$\|V(x,t)\|^2_{L^2(0,T;L^2(\Omega))} \le \varepsilon^4\|v(x,t)\|^2_{L^2(0,T/\varepsilon^2;L^2(\Omega))} \le CT\varepsilon^6|\log\varepsilon|,$$
$$\|\nabla_x V(x,t)\|^2_{L^2(0,T;L^2(\Omega))} \le \varepsilon^2\|\nabla_x v(x,t)\|^2_{L^2(0,T/\varepsilon^2;L^2(\Omega))} \le CT\varepsilon^4|\log\varepsilon|,$$

as desired. □

5. The resulting expansion after multiplication by a test function and integration on the surface plane

Suppose that the space dimension is 3. Let Φ be in $L^2(0,T;H^1(\Omega))$ such that

$$(\partial_t+\Delta)\Phi = 0 \ \text{ in } \Omega\times(0,T), \tag{5.1}$$
$$\Phi(.,T) = 0. \tag{5.2}$$

Let v_ε satisfy (3.8)-(3.13). We find by integration by parts and application of Theorem 3.2,

$$\int_0^T\int_{\partial\Omega} v_\varepsilon\Big(\frac{\partial\Phi}{\partial x_3}+\Phi\Big)$$
$$= \varepsilon^3\sum_{j=1}^m\Big(\frac{k_j}{k_0}-1\Big)\int_0^T\sum_{i=1}^3\partial_{x_i}u_0(z_j,t)\int_{B_j}\nabla\psi_{j,i}(x)\nabla\Phi(z_j,t)+R, \tag{5.3}$$

where the remainder R is bounded by

$$|R| \le CT\varepsilon^4 \sup_{D\times(0,T)}|\nabla\Phi|.$$

A calculation shows that $(\int_{B_j} \nabla\psi_{j,i}(x))_{i=1,\cdots,3}$ can be replaced by the polarization tensor $M^{(j)}$ (depending only on B_j and k_j/k_0) to obtain

$$\begin{aligned}&\int_0^T \int_{\partial\Omega} v_\varepsilon \Big(\frac{\partial\Phi}{\partial x_3} + \Phi\Big)\\ &= \varepsilon^3 \sum_{j=1}^m \Big(\frac{k_j}{k_0} - 1\Big) \int_0^T \nabla u_0(z_j,t) M^{(j)} \nabla\Phi(z_j,t) + R. \end{aligned} \tag{5.4}$$

In the two-dimensional case, the cut off section appearing in formula (4.6) goes away by integration on a bounded set. We obtain,

$$\begin{aligned}&\int_0^T \int_{\partial\Omega} v_\varepsilon \Big(\frac{\partial\Phi}{\partial x_2} + \Phi\Big)\\ &= \varepsilon^2 \sum_{j=1}^m \Big(\frac{k_j}{k_0} - 1\Big) \int_0^T \nabla u_0(z_j,t) M^{(j)} \nabla\Phi(z_j,t) + R, \end{aligned} \tag{5.5}$$

for Φ satisfying (5.1)-(5.2), and where R is bounded by

$$|R| \le C T \varepsilon^3 |\log\varepsilon|^{\frac{1}{2}} \sup_{D\times(0,T)} |\nabla\Phi|.$$

It is worth mentioning that the concept of the polarization tensor has been used in various area such as the imaging of small anomalies and the effective medium theory. We refer the reader to the recent book [6] for an extensive study of its properties.

We summarize in the following theorem our main results in this paper.

Theorem 5.1. **(i)** *The following asymptotic expansions for the weighted boundary measurements hold:*

$$\begin{aligned}\int_0^T \int_{\partial\Omega} (u_\varepsilon - u_0)\Big(\frac{\partial\Phi}{\partial x_d} + \Phi\Big) &= \varepsilon^d \sum_{j=1}^m \Big(\frac{k_j}{k_0} - 1\Big) \int_0^T \nabla u_0(z_j,t) M^{(j)} \nabla\Phi(z_j,t)\\ &+ \begin{cases} \mathcal{O}\left(T\varepsilon^4 \sup_{D\times(0,T)} |\nabla\Phi|\right) & \text{for } d=3,\\ \mathcal{O}\left(T\varepsilon^3 |\log\varepsilon|^{\frac{1}{2}} \sup_{D\times(0,T)} |\nabla\Phi|\right) & \text{for } d=2. \end{cases}\end{aligned}$$

(ii) *The following inner expansions hold. We have in the two-dimensional case*

$$\begin{aligned}&\Big\| u_\varepsilon - u_0 + \varepsilon \sum_{j=1}^m \sum_{i=1}^2 \partial_{x_i} u_0(z_j,t) \psi_{j,i}\Big(\frac{x - z_j}{\varepsilon}\Big) \rho(\varepsilon x) \Big\|_{L^2(0,T;H^1(\Omega))}\\ &\le C T^{\frac{1}{2}} \varepsilon^2 |\log\varepsilon|^{\frac{1}{2}},\end{aligned}$$

where $\rho \in \mathscr{C}^\infty(\mathbb{R}^2)$ is such that $\rho(x) = 1$ if $|x| \leq 1, \rho(x) = 0$ if $|x| \geq 2$, while in three dimensions

$$\left\| u_\varepsilon - u_0 + \varepsilon \sum_{j=1}^{m} \sum_{i=1}^{2} \partial_{x_i} u_0(z_j, t) \psi_{j,i}\Big(\frac{x - z_j}{\varepsilon}\Big) \right\|_{L^2(0,T;H^1(\Omega))} \leq C T^{\frac{1}{2}} \varepsilon^{\frac{5}{2}}.$$

The weighted boundary measurements will be used in the next section to design non-iterative algorithms for detecting the anomalies from boundary measurements while the inner expansions form the basis of the reconstruction method from ultrasonic thermal measurements. The inner expansions allow to reconstruct the anomalies with much better spatial and contrast resolutions than the weighted measurements which only gives the location and of some geometric features of the anomaly. In fact, the inner expansions uniquely characterize the shape and the thermal conductivity of the anomaly. In contrast, the asymptotic expansions of the weighted measurements show that, from an imaging point of view, the location and the polarization tensor of the anomaly are the only quantities that can be determined from boundary measurements.

6. Examples of applications

6.1. Active temperature imaging

In this section we examine the two dimensional case ($d = 2$), and assume that all the anomalies are disks. These assumptions are made only for ease of exposition: other cases can be worked out equally well. In particular, if the anomalies have non trivial shapes, the only complication stems from the polarization tensor which is no longer proportional to the identity matrix. Accordingly, the analysis becomes slightly more involved in that case. However, in that case too, anomalies can be detected and their polarization tensors can be estimated.

Choose $u_{ext} = \delta_{t=0}\delta_y$ for some point $y \in \partial\Omega$ and $u_{init} = 0$ in Ω. The unperturbed solution corresponds to $u_0(x,t) = G_2(x,y,t)$. Choose $\Phi(x,t) = G_2(x,y',T-t)$, where $y' \in \partial\Omega$. The asymptotic formula for the weighted boundary measurements yields

$$(u_\varepsilon - u_0)(y',T) \approx 2\varepsilon^2 \sum_{j=1}^{m} (k_j/k_0 - 1) \frac{|B_j|}{1 + k_j/k_0} \int_0^T \nabla G_2(z_j, y, t) \cdot \nabla G_2(z_j, y', T-t) dt.$$

Let now $y, y' \in \{y_1, \cdots, y_n\}$, where $y_1, \cdots, y_n$ are source points on $\partial\Omega$. Define the matrix $A = \{A_{ll'}\}_{l,l'=1}^n$ by

$$A_{ll'} := 2\varepsilon^2 \sum_{j=1}^{m} (k_j/k_0 - 1) \frac{|B_j|}{1 + k_j/k_0} \int_0^T \nabla G_2(z_j, y_l, t) \cdot \nabla G_2(z_j, y_{l'}, T-t) dt.$$

For $z \in \Omega$, we define the real symmetric matrix C by

$$C := \left[\int_0^T \nabla G_2(z, y_l, t) \cdot \nabla G_2(z, y_{l'}, T-t) dt \right]_{l,l'=1,\cdots,n}$$

and we rewrite C in terms of its eigenvectors

$$C = \sum_{l=1}^{p} v_l(z) v_l^*(z)$$

for some $p \leq n$, where v_l^* denotes the transpose of v_l. By exactly the same arguments as those in [4], the following characterization of the range of the matrix A holds:

$$v_l(z) \in \text{Range}(A)\ \forall l \in \{1, \cdots, p\} \text{ iff } z \in \{z_1, \cdots, z_m\},$$

for all sufficiently large number of source points n. Let the singular value decomposition (SVD) of the matrix A be defined by $A = U\Sigma V^*$. Let U_{signal} denote the first columns of U that provide a basis for the column space of A and U_{noise} the rest of the matrix U which provides a basis for the left null space of A. From the characterization of the range of A, a test point z coincides with one of the locations z_j if and only if $P(v_l(z)) = 0$, where

$$P = I - U_{signal} U_{signal}^*$$

is the orthogonal projection onto the null space of A. Thus we can form an image of the locations $\{z_j\}_{j=1}^m$ by plotting, at each z in a box search, the quantities

$$W_l(z) := \frac{1}{||P(v_l(z))||} \quad \text{for } l = 1, \cdots, p.$$

The resulting plot will have large peaks at the locations of $z_j, j = 1, \cdots, m$.

The matrix A is known from measurements of $(u_\varepsilon - u_0)(y', T)$, where $u_0(x,t) = G_2(x,y,t)$ and $y, y' \in \{y_1, \cdots, y_n\}$.

Other choices for heating are possible. For example, we can place the heat source in the upper half space by choosing

$$u_{ext}(x,t) = \frac{1}{t}\left[\exp\Big(-\frac{|x-y|^2}{4t}\Big) + \frac{\partial}{\partial x_2} \exp\Big(-\frac{|x-y|^2}{4t}\Big)\right] \quad \text{for } x \in \partial\Omega,$$

and $y \in \mathbb{R}^2 \setminus \Omega$. Then we take

$$\Phi(x,t) = \frac{1}{(T-t)} \exp\Big(-\frac{|x-y|^2}{4(T-t)}\Big),$$

for $y' \in \mathbb{R}^2 \setminus \Omega$ and $u_{init} = 0$ in Ω. Set $y, y' \in \{y_1, \cdots, y_n\}$, where $y_l \in \mathbb{R}^2 \setminus \overline{\Omega}$. Construct the matrix A from the weighted measurements

$$\int_0^T \int_{\partial\Omega} (u_\varepsilon - u_0)\Big(\frac{\partial \Phi}{\partial x_d} + \Phi\Big).$$

The same imaging algorithm applies when $v_l(z)$ is constructed from the decomposition of the matrix

$$\left[\int_0^T \nabla G(z, y_l, t) \cdot \nabla G(z, y_{l'}, T-t) dt\right]_{l,l'=1,\cdots,n},$$

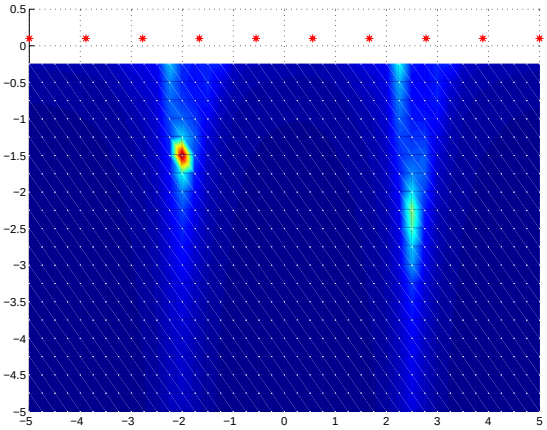

Figure 1: Detection of anomalies.

where

$$G(z,y,t)=\frac{1}{t}\exp\Big(-\frac{|z-y|^2}{4t}\Big).$$

Because of the singularity of G_2 on the boundary $\partial\Omega$, the second choice of heating is easier to implement numerically.

In the following example, two anomalies of radius 0.3 and 0.1 and conductivities 2 and 5 are placed at $(-2,-1.5)$ and $(2.5,-2.5)$, respectively. We set $T=1$ and the conductivity of the background equals to 0.1. We choose $n=10$ heat sources placed at the same $x_2>0$ and at $x_1^l=-5+10(l-1)/9, l=1,\cdots,10$. The next two figures show the reconstructions without and with noise.

In Fig. 1, we see clearly the presence of two anomalies. However, the one on the right, which is also deeper, is not as well rendered as the one on the left.

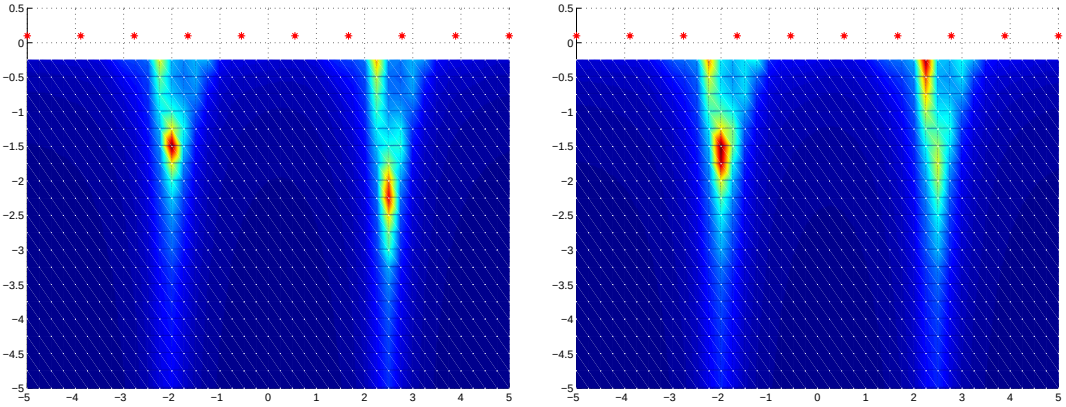

Figure 2: Detection in the presence of 1% (on the left) and 5% (on the right) of noise.

6.2. Passive temperature imaging

This appears to be a harder problem as no forcing can be imposed. The process is passive and driven by cooling. Choose u_{init} in the form $e^{\alpha x_3}$, $\alpha > 0$ and u_{ext} linear in time to simulate cooling: $u_{ext}(x,t) = 1 + \alpha - \beta t$, for $x \in \partial\Omega$.

The unperturbed solution $u_0(x,t)$ has the following form:

$$u_0(x_1,\cdots,x_d,t) = \int_{-\infty}^{0} \widetilde{u}_{init}(\xi_d)\widetilde{G}_1(x_d,\xi_d,t)d\xi_d + \int_0^t \widetilde{u}_{ext}(s)\widetilde{G}_2(x_d,t-s)ds, \tag{6.1}$$

where $\widetilde{G}_1(x_d,\xi_d,t)$ is given by

$$\widetilde{G}_1(x_d,\xi_d,t) = \frac{1}{\sqrt{4\pi t}}\left(e^{-\frac{(x_d-\xi_d)^2}{4t}} + e^{-\frac{(x_d+\xi_d)^2}{4t}} - 2\int_0^{+\infty} e^{-\frac{(x_d+\xi_d-\eta)^2}{4t}-\eta}d\eta\right), \tag{6.2}$$

and $\widetilde{G}_2(x_d,t) = \widetilde{G}_1(x_d,0,t)$.

It is easy to see that the gradient of unperturbed solution u_0 has only one nontrivial component:

$$\nabla_x u_0(x,t) = \begin{pmatrix} 0 \\ \vdots \\ \int_{-\infty}^{0} \widetilde{u}_{init}(\xi_d)\frac{\partial\widetilde{G}_1}{\partial x_d}(x_d,\xi_d,t)d\xi_d + \int_0^t \widetilde{u}_{ext}(s)\frac{\partial\widetilde{G}_2}{\partial x_d}(x_d,t-s)ds \end{pmatrix}. \tag{6.3}$$

Suppose for the sake of simplicity that $d = 2$ and all the anomalies are disks. For $y = (y_1,y_2)$ in the upper half-space, choose

$$\Phi(x,t) = \Phi(x,y,t,T) := \frac{1}{(T-t)}\exp\Big(-\frac{|x-y|^2}{4(T-t)}\Big),$$

as in the above section. For $j = 1,\cdots,m$, write $z_j = (z_j^{(1)}, z_j^{(2)})$. We see from Theorem 5.1 that for fixed y_2 the functional

$$I_\Phi(T) := \int_0^T \int_{\partial\Omega} (u_\varepsilon - u_0)\Big(\frac{\partial\Phi}{\partial x_d} + \Phi\Big)$$

has extrema for $y_1 = z_j^{(1)}, j = 1,\cdots,m$.

To verify the validity the asymptotic expansion in Theorem 5.1, we compare the values of $I_\Phi(T)$ as a function of y_1 computed directly with those given by the asymptotic formula. Here $y_2 = 0.1$ and $T = 0.1$. Fig. 3 shows these comparisons for an inclusion located at $(-2,-1.5)$ with different radius $(0.005, 0.01, 0.1$ and $0.2)$ and different thermal

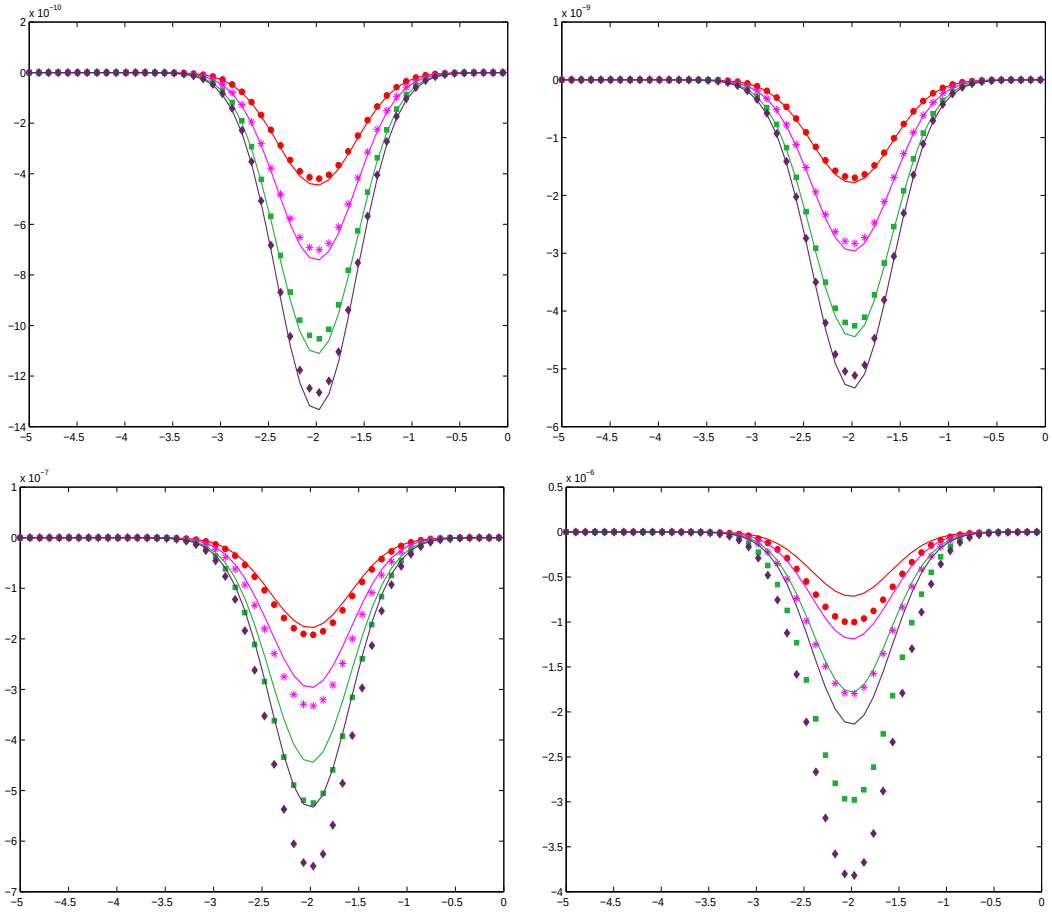

Figure 3: Validation of the asymptotic expansion formula for inclusions with different radius and thermal conductivities. From top to bottom, from left to right: the radius of the inclusion is 0.005, 0.01, 0.1 and 0.2. In each figure, the conductivities are from the top to the bottom: $1.5, 2, 3$, and 4.

conductivities $1.5, 2, 3$ and 4. The approximation error gets larger with the radius of the anomaly.

As we can see from Fig. 3, the first order of magnitude given by the asymptotic expansion formula is valid for the anomalies of radius 0.005 and 0.01. In contrast, for the anomalies of radius 0.1 and 0.2 there is a significant error.

It is verified on Fig. 4 that the extrema of $I_\Phi(T)$ correspond to the x_1 components of the locations of the anomalies.

Once the x_1 components, $z_j^1, j = 1, \cdots, m$, are found, in order to recover the x_2 components we minimize over $z_j^2 < 0, j = 1, \cdots, m$, the following functional

$$\left| I_\Phi(T) - \varepsilon^2 \sum_{j=1}^{m} (k_j/k_0 - 1) \int_0^T \nabla u_0((z_j^1, z_j^2), t) M^{(j)} \nabla \Phi((z_j^1, z_j^2), t) dt \right|.$$

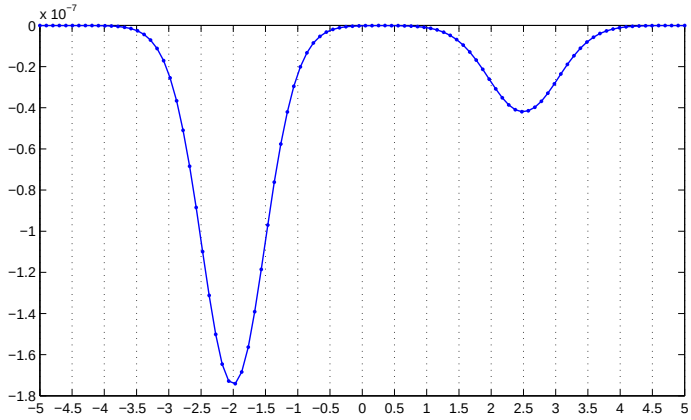

Figure 4: Reconstruction of the anomalies.

6.3. Ultrasonic temperature imaging

The idea behind ultrasonic temperature imaging hinges on measuring local temperature near anomalies. The aim is to reconstruct anomalies with higher spatial and contrast resolution as compared to those obtained from boundary measurements alone. Theorem 5.1 expresses that the following approximation is valid

$$(u_\varepsilon - u_0)(x,t) \approx -\varepsilon \sum_{i=1}^{2} \partial_{x_i} u_0(z_{j_0},t)\psi_{j,i}\Big(\frac{x-z_{j_0}}{\varepsilon}\Big),$$

for $|x - z_{j_0}| = \mathcal{O}(\varepsilon)$. Fix ω to be a window around the anomaly j_0. To reconstruct the shape and the thermal conductivity of this anomaly, a natural way to proceed would be to minimize over εB and k the functional

$$\int_0^T \int_\omega \Big|(u_\varepsilon - u_0)(x,t) + \varepsilon \sum_{i=1}^{2} \partial_{x_i} u_0(z_{j_0},t)\psi_{j,i}\Big(\frac{x-z_{j_0}}{\varepsilon}\Big)\Big|^2 dx dt.$$

Standard regularization techniques may help for solving this optimization problem. See [3].

7. Concluding remarks

In this paper, starting from a realistic half space model for thermal imaging, we have developed a mathematical asymptotic analysis well suited for the design of reconstruction algorithms. Based on rigorously derived asymptotic estimates, after obtaining an approximation for the temperature profile, we were able to design noniterative detection algorithms. We have then presented numerical simulations to test them. These algorithms are based on either heating generated by point sources on the surface of the medium, or

cooling of the medium modeled by a uniform convective condition on the surface. Both these algorithms can be applied to medical thermal imaging. Since they are solely based on observing quantities which are only "singular" at the locations of the anomalies, we can claim that these algorithms are not overly sensitive to observation noise. See [5] for a general discussion of sensitivity to noise for this type of reconstruction algorithm.

We have also touched upon the subject of ultrasonic temperature imaging used for guiding in the course of thermal ablation therapy. Related optimization algorithms will be the subject of forthcoming work.

Acknowledgments This research was partially supported by the ANR project EchoScan (AN-06-Blan-0089) and the NSF grant DMS 0707421.

Appendix

We derive Eqs. (4.3)-(4.5) from (4.2), if f_2 is in $L^2((0,T)\times\mathbb{R})$ and

$$\lim_{\varepsilon\to 0}\int_{0\le s\le\varepsilon}\int_{|y|\le\varepsilon}|f_2(x+y,t-s)-f_2(x,t)|dyds=0. \tag{A.1}$$

Eq. (4.3) is clear by dominated convergence. Eq. (4.5) can be obtained for any $x_2<0$ by applying Cauchy Schwartz inequality and letting t tend to 0.

To obtain (4.4), first assume that f_2 is equal to the constant 1 in the neighborhood of (x_1,t) defined by $|\xi_1-x_1|<\eta, |s-t|<\eta$. We observe the following, due to the boundary condition for G_2 away from singularities,

$$\lim_{x_2\to 0}(\partial_{x_2}\cdot+\cdot)\left(\iint_X f_2(\xi_1,s)G_2(x_1,x_2,\xi_1,t-s)d\xi_1 ds\right)=0,$$

where X is the complement in $(0,t)\times\mathbb{R}$ of $(t-\eta,t)\times(x_1-\eta,x_1+\eta)$. Next we set for $x_2<0$, $u=\xi_1-x_1$, $r=s-t$. We want to determine

$$\lim_{x_2\to 0}(\partial_{x_2}\cdot+\cdot)\left(\int_0^\eta\int_{-\eta}^\eta G_2(u,x_2,0,r)dudr\right).$$

Note that

$$\begin{aligned}&G_2(u,x_2,0,r)\\&=\frac{1}{4}e^{-\frac{u^2}{4r}}\left(2\,e^{\frac{{x_2}^2}{4r}}+2\sqrt{\pi}e^{-x_2+r}\sqrt{r}\left(erf\left(\frac{1}{2}\frac{-x_2+2r}{\sqrt{r}}\right)-1\right)\right)\pi^{-1}r^{-1}.\end{aligned}$$

Integrating the above equation with respect to u gives

$$\begin{aligned}\int_{-\eta}^{\eta}G_2(u,x_2,0,r)du&=e^{\frac{{x_2}^2}{4r}}erf\left(\frac{\eta}{2\sqrt{r}}\right)\frac{1}{\sqrt{\pi}}\frac{1}{\sqrt{r}}\\&\quad+e^{-x_2+r}erf\left(\frac{-x_2+2r}{2\sqrt{r}}\right)erf\left(\frac{\eta}{2\sqrt{r}}\right)-e^{-x_2+r}erf\left(\frac{\eta}{2\sqrt{r}}\right).\end{aligned}$$

We can let x_2 tend to zero in the latter expression, since dominated convergence can be applied. Next, since

$$\partial_{x_2} G_2(u,x_2,0,r) = \frac{1}{4\pi}\, e^{\frac{u^2}{4r}} \Bigg[-x_2 e^{\frac{{x_2}^2}{4r}} r^{-2} \\ -2\sqrt{\pi} e^{-x_2+r} r^{-1/2} \Big(erf\big(\frac{-x_2+2r}{2\sqrt{r}}\big) - 1 \Big) - 2\, e^{-x_2+r} e^{\frac{(-x_2+2r)^2}{4r}} r^{-1} \Bigg],$$

we notice that $\partial_{x_2} G_2(u,x_2,0,r)$ is the sum of three terms, the most singular is of order r^{-2}, the other two are of order, respectively, r^{-1} and $r^{-1/2}$. Starting with the most singular term, integrating in u,

$$\int_{-\eta}^{\eta} \frac{1}{4\pi}\, e^{\frac{u^2}{4r}} (-x_2) e^{\frac{{x_2}^2}{4r}} r^{-2} du = -\frac{1}{2}\, x_2 e^{\frac{{x_2}^2}{4r}} erf\left(\frac{\eta}{2\sqrt{r}}\right) \frac{1}{\sqrt{\pi}} r^{-3/2}.$$

To proceed with the integration in r, we make the substitution $r = s^{-2} x_2^2$ to obtain the integral

$$\int_{x_2^2/\eta^2}^{\infty} -e^{-1/4s^2} erf\left(\frac{s\eta}{2x_2}\right) \frac{1}{\sqrt{\pi}} ds.$$

By dominated convergence, the latter has the limit, as $x_2 < 0$ approaches 0,

$$\int_0^{\infty} e^{-1/4s^2} \frac{1}{\sqrt{\pi}} ds,$$

which is equal to 1. We now examine the two terms from $\partial_{x_2} G_2(u,x_2,0,r)$, of lower order in r. Integrating in u,

$$\int_{-\eta}^{\eta} \frac{1}{4\pi}\, e^{\frac{u^2}{4r}} \Bigg[-2\sqrt{\pi} e^{-x_2+r} r^{-1/2} \Big(erf\big(\frac{-x_2+2r}{2\sqrt{r}}\big) - 1 \Big) - 2\, e^{-x_2+r} e^{\frac{(-x_2+2r)^2}{4r}} r^{-1} \Bigg] du \\ = e^{-x_2+r} erf\left(\frac{-x_2+2r}{2\sqrt{r}}\right) erf\left(\frac{\eta}{2\sqrt{r}}\right) - e^{-x_2+r} erf\left(\frac{\eta}{2\sqrt{r}}\right) - e^{\frac{{x_2}^2}{4r}} erf\left(\frac{\eta}{2\sqrt{r}}\right) \frac{1}{\sqrt{\pi r}}.$$

We can let x_2 tend to zero in the latter expression, since dominated convergence can be applied. In conclusion,

$$\lim_{x_2 \to 0} (\partial_{x_2} \cdot + \cdot) \left(\int_0^t \int_{-\infty}^{\infty} f_2(\xi_1, s) G_2(x_1, x_2, \xi_1, t-s) d\xi_1 ds \right) = 1,$$

if f_2 is equal to the constant 1 in some neighborhood of (x_1, t). The more general case can then be obtained by playing with inequalities, starting from estimate (A.1).

References

[1] W.C. Amalu, W.B. Hobbins, and R.L. Elliot, *Infrared imaging of the breast–An overview*, Chap. 25 in *Medical Devices and Systems*, The Biomedical Engineering Handbook, 3rd Ed., ed. by J.D. Bronzino, CRC Press, 2006.

[2] H. Ammari, *An Introduction to Mathematics of Emerging Biomedical Imaging*, Math & Appl., Vol. 62, Springer-Verlag, Berlin, 2008.

[3] H. Ammari, P. Garapon, H. Kang, and H. Lee, *A method of biological tissues elasticity reconstruction using magnetic resonance elastography measurements*, Quart. Appl. Math., 66 (2008), pp. 139–175.

[4] H. Ammari, E. Iakovleva, H. Kang, and K. Kim, *A direct algorithm for thermal imaging of small inclusions*, SIAM J. Mult. Model. Simul., 4 (2005), pp. 1116–1136.

[5] H. Ammari and H. Kang, *Reconstruction of Small Inhomogeneities from Boundary Measurements,* Lecture Notes in Mathematics, Vol. 1846, Springer-Verlag, Berlin, 2004.

[6] H. Ammari and H. Kang, *Polarization and Moment Tensors with Applications to Inverse Problems and Effective Medium Theory*, Applied Mathematical Sciences, Vol. 162, Springer-Verlag, New York, 2007.

[7] H. Ammari, O. Kwon, J.K. Seo, and E.J. Woo, *T-scan electrical impedance imaging system for anomaly detection*, SIAM J. Appl. Math., 65 (2005), pp. 252–266.

[8] H. Brezis, *Analyse Fonctionnelle: Théorie et Applications*, Masson, Paris, 1992.

[9] J.H. Lienhard IV and J.H. Lienhard V, *A Heat Transfer Textbook*, Phlogiston Press, Cambridge, Massachusetts, 2006.

[10] J.C. Lantis II, K.L. Carr, R. Grabowy, R.J. Connolly, and S.D. Schwaitzberg,*Microwave applications in clinical medicine*, Surg Endosc, 12 (1998), pp. 170Ű-176.

[11] J.L. Lions, *Equations Différentielles Opérationnelles et Problèmes aux Limites*, Springer-Verlag, Berlin, 1961.

[12] N.R. Miller, J.C. Bamber, and G.R. ter Haar, *Ultrasonic temperature imaging for the guidance of thermal ablation therapies: in vitro results*, 2002 IEEE Ultrasonic Symposium, pp. 1365–1368.

[13] Y.R. Parisky, A. Sardi, R. Hamm, K. Hughes, L. Esserman, S. Rust, and K. Callahan, *Efficacy of computerized infrared imaging analysis to evaluate mammographically suspicious lesions*, American J. Radiology, 180 (2003), pp. 263–269.

[14] A. Sommerfeld, *Partial Differential Equations in Physics*, Academic Press, New York, 1949.

[15] T. Yahara, T. Koga, S. Yoshida, S. Nakagawa, H. Deguchi, and K. Shirouzu, *Relationship between microvessel density and thermographic hot areas in breast cancer*, Surg Today, 33 (2003), pp. 243–248.